Published in final edited form as:
Annu Rev Biochem. 2009 ; 78: 993–1016. doi:10.1146/annurev.biochem.77.061906.092014.

Super resolution fluorescence microscopy

Bo Huang[1,2], **Mark Bates**[3], and **Xiaowei Zhuang**[1,2,4]

Bo Huang: bohuang@fas.harvard.edu; Mark Bates: bates@fas.harvard.edu; Xiaowei Zhuang: zhuang@chemistry.harvard.edu

[1]Howard Hughes Medical Institute, Harvard University, Cambridge, Massachusetts 02138

[2]Department of Chemistry and Chemical Biology, Harvard University, Cambridge, Massachusetts 02138

[3]School of Engineering and Applied Sciences, Harvard University, Cambridge, Massachusetts 02138

[4]Department of Physics, Harvard University, Cambridge, Massachusetts 02138

Abstract

Achieving a spatial resolution that is not limited by the diffraction of light, recent developments of super-resolution fluorescence microscopy techniques allow the observation of many biological structures not resolvable in conventional fluorescence microscopy. New advances in these techniques now give them the ability to image three-dimensional (3D) structures, measure interactions by multicolor colocalization, and record dynamic processes in living cells at the nanometer scale. It is anticipated that super-resolution fluorescence microscopy will become a widely used tool for cell and tissue imaging to provide previously unobserved details of biological structures and processes.

Keywords

Sub-diffraction limit; single-molecule; multicolor imaging; three-dimensional imaging; live cell imaging; single-particle tracking; photoswitchable probe

INTRODUCTION

Much of our knowledge regarding biological processes at the cellular and subcellular level has come from the ability to directly visualize them. Among the various microscopy techniques, fluorescence microscopy is one of the most widely used because of its two principal advantages: Specific cellular components may be observed through molecule-specific labeling, and light microscopy allows the observation of structures inside a live sample in real time. Compared to other imaging techniques such as electron microscopy (EM), however, conventional fluorescence microscopy is limited by relatively low spatial resolution because of the diffraction of light. This diffraction limit, about 200–300 nm in the lateral direction and 500–700 nm in the axial direction, is comparable to or larger than many subcellular structures, leaving them too small to be observed in detail. In recent years, a number of "super-resolution" fluorescence microscopy techniques have been invented to overcome the diffraction barrier, including techniques that employ nonlinear effects to sharpen the point-spread function of the microscope, such as stimulated emission depletion (STED) microscopy (1,2), related methods

Disclosure Statement

The authors are not aware of any affiliations, memberships, funding, or financial holdings that might be perceived as affecting the objectivity of this review.

using other reversible saturable optically linear fluorescence transitions (RESOLFTs) (3), and saturated structured-illumination microscopy (SSIM) (4), as well as techniques that are based on the localization of individual fluorescent molecules, such as stochastic optical reconstruction microscopy (STORM) (5), photoactivated localization microscopy (PALM) (6), and fluorescence photoactivation localization microscopy (FPALM) (7). These methods have yielded an order of magnitude improvement in spatial resolution in all three dimensions over conventional light microscopy. The observation of previously unresolved details of cellular structures has demonstrated the great promise of super-resolution fluorescence microscopy in elucidating biological processes at the cellular and molecular scale.

In this review, we summarize the current state of development and future challenges of super-resolution fluorescence microscopy techniques, as well as their application to the study of biological problems.

THE RESOLUTION LIMIT IN OPTICAL MICROSCOPY

Microscopes can be used to visualize fine structures in a sample by providing a magnified image. However, even an arbitrarily high magnification does not translate into the ability to see infinitely small details. Instead, the resolution of light microscopy is limited because light is a wave and is subject to diffraction.

The diffraction limit

An optical microscope can be thought of as a lens system that produces a magnified image of a small object. In this imaging process, light rays from each point on the object converge to a single point at the image plane. However, the diffraction of light prevents exact convergence of the rays, causing a sharp point on the object to blur into a finite-sized spot in the image. The three-dimensional (3D) intensity distribution of the image of a point object is called the point spread function (PSF). The size of the PSF determines the resolution of the microscope: Two points closer than the full width at half-maximum (FWHM) of the PSF will be difficult to resolve because their images overlap substantially.

The FWHM of the PSF in the lateral directions (the x–y directions perpendicular to the optical axis) can be approximated as $\Delta xy \approx 0.61\lambda / \mathrm{NA}$, where λ is the wavelength of the light, and NA is the numerical aperture of the objective defined as $\mathrm{NA} = n \sin\alpha$, with n being the refractive index of the medium and α being the half-cone angle of the focused light produced by the objective. The axial width of the PSF is about 2–3 times as large as the lateral width for ordinary high NA objectives. When imaging with visible light ($\lambda \approx 550$ nm), the commonly used oil immersion objective with NA = 1.40 yields a PSF with a lateral size of ~200 nm and an axial size of ~500 nm in a refractive index-matched medium (Figure 1) (8).

The diffraction limit of resolution in light microscopy does not affect most imaging at the organ or tissue level. However, when zooming into cells, where a large number of subcellular structures are smaller than the wavelength of the light, it becomes an obstacle for studying these structures in detail. It is, therefore, important to develop techniques that improve the spatial resolution of light microscopy without compromising its noninvasiveness and biomolecular specificity.

Because the loss of high-frequency spatial information in optical microscopy results from the diffraction of light when it propagates through a distance larger than the wavelength of the light (far field), near-field microscopy is one of the earliest approaches sought to achieve high spatial resolution. By exciting the fluorophores or detecting the signal through the nonpropagating light near the fluorophore, high-resolution information be retained. Near-field scanning optical microscopy (NSOM) acquires an image by scanning a sharp probe tip across

the sample, typically providing a resolution of 20–50 nm (9–11). Wide-field imaging has also been recently demonstrated in the near-field regime using a super lens with negative refractive index (12,13). However, the short range of the near-field region (tens of nanometers) compromises the ability of light microscopy to look into a sample, limiting the application of near-field microscopy to near-surface features only. This limit highlights the need to develop far-field high-resolution imaging methods.

Extended resolution in optical microscopy

Several far-field imaging methods are known to extend the diffraction-limited resolution to smaller values.

Confocal and multiphoton microscopy—Among far-field fluorescence microscopy techniques, confocal and multiphoton microscopy are among the most widely used to moderately enhance the spatial resolution (14,15). By combining a focused laser for excitation and a pinhole for detection, confocal microscopy can, in principle, have a factor of $\sqrt{2}$ improvement in the spatial resolution. In multiphoton microscopy, nonlinear absorption processes reduce the effective size of the excitation PSF. However, this gain in the PSF size is counteracted by the increased wavelength of the excitation light. Thus, instead of improving the resolution, the main advantage of confocal and multiphoton microscopy over wide-field microscopy is the reduction of out-of-focus fluorescence background, allowing optical sectioning in 3D imaging.

4Pi microscopy and I^5M—Because microscope objectives collect light from only one side of the sample, a large amount of light is lost, leading to a PSF that is elongated in the axial direction. One can imagine that if the full spherical angle could be covered by the objective, the PSF would become symmetric with the axial size being the same as the lateral size. Two techniques, 4Pi and I5M microscopy, approach this ideal situation by using two opposing objectives for excitation and/or detection (16,17). This effective increase in NA boosts the lateral resolution by a modest amount, but substantially improve the axial resolution to ~100 nm.

Structured Illumination Microscopy (SIM)—Another approach to increase the spatial resolution of optical microscopy is to apply a patterned illumination field to the sample. In this approach, the spatial frequencies of the illumination pattern mix with those of the sample features, shifting the high-frequency features to lower frequencies that are detectable by the microscope. Periodic illumination patterns can be created through the interference of multiple light sources in the axial direction (18), the lateral direction (19), or both (20). By acquiring multiple images with illumination patterns of different phases and orientations, a high-resolution image can be reconstructed. Because the illumination pattern itself is also limited by the diffraction of light, structured illumination microscopy (SIM) is only capable of doubling the spatial resolution by combining two diffraction-limited sources of information. A resolution of~100 nm in the lateral direction and ~300 nm in the axial direction has been achieved (19–21).

The extended diffraction limit of resolution—The advantage of these purely optical approaches is that they are not dependent on any special photophysics or photochemistry of the fluorophore; therefore, virtually any fluorescent probe can be used. The best achievable result using these methods would be an isotropic PSF with an additional factor of 2 in resolution improvement. This would correspond to ~100-nm image resolution in all three dimensions, as has been demonstrated by the I5S technique, which combines I5M and SIM (22). Albeit a significant improvement, this resolution is still fundamentally limited by the diffraction of light. To break the diffraction limit and obtain much higher image resolution would need

additional factors, in particular the involvement of fluorophore photophysics or photochemistry.

SUPER RESOLUTION FLUORESCENCE MICROSCOPY BY SPATIALLY PATTERNED EXCITATION

One approach to attain a resolution far beyond the limit of diffraction, i.e., to realize super-resolution microscopy, is to introduce sub-diffraction-limit features in the excitation pattern so that small-length-scale information can be read out. We refer to this approach, including STED, RESOLFT, and SSIM, as super-resolution microscopy by spatially patterned excitation or the "patterned excitation" approach.

Stimulated emission depletion (STED) microscopy

The concept of STED microscopy was first proposed in 1994 (1) and subsequently demonstrated experimentally (2). Simply speaking, it uses a second laser (STED laser) to suppress the fluorescence emission from the fluorophores located off the center of the excitation. This suppression is achieved through stimulated emission: When an excited-state fluorophores encounters a photon that matches the energy difference between the excited and the ground state, it can be brought back to the ground state through stimulated emission before spontaneous fluorescence emission occurs. This process effectively depletes excited-state fluorophores capable of fluorescence emission (Figure 2a,b).

In order to use STED to sharpen the excitation PSF, the STED laser needs to have a pattern with zero intensity at the center of the excitation laser focus and nonzero intensity at the periphery. However, this spatial pattern is also limited by the diffraction of light. Therefore, the effect of STED alone is not sufficient for sub-diffraction-limit imaging. The key to achieving super resolution is the nonlinear dependence of the depleted population on the STED laser intensity when the saturated depletion level is approached: If the local intensity of the STED laser is higher than a certain level, essentially all spontaneous fluorescence emission is suppressed. By raising the STED laser power, the saturated depletion region expands without strongly affecting fluorescence emission at the focal point because the STED laser intensity is nearly zero at this point. Consequently, the fluorescence signal can be observed only in a small region around the focal point, reducing the effective width of the PSF (Figure 2c). The size of this region is limited by the practical power level of the STED laser instead of the diffraction of light. Super-resolution images are then obtained by scanning this small effective PSF.

The pattern of the STED laser is typically generated by inserting a phase mask into the light path to modulate its phase-spatial distribution (Figure 2b). One such phase mask generates a donut-shaped STED pattern in the *xy* plane (Figure 2c) and has provided an *xy* resolution of ~30 nm (24). STED can also be employed in 4Pi microscopy (STED-4Pi), resulting in an axial resolution of 30–40 nm (25). STED has been applied to biological samples either immunostained with fluorophorelabeled antibodies (26) or genetically tagged with fluorescent proteins (FPs) (27). Dyes with high photostability under STED conditions and large stimulated emission cross sections in the visible to near infrared (IR) range are preferred. Atto 532 and Atto 647N are among the most often used dyes for STED microscopy.

A more general concept: RESOLFT

Stimulated emission is not the only mechanism capable of suppressing undesired fluorescence emission. A more general scheme using saturable depletion to achieve super resolution has been formalized with the name RESOLFT microscopy (3). This scheme employs fluorescent probes that can be reversibly photoswitched between a fluorescent on state and a dark off state. The off state can be the ground state of a fluorophores as in the case of STED, the triplet state

as in ground-state-depletion microscopy (28,29), or the dark state of a reversibly photoswitchable fluorophore (30). The gain in spatial resolution is achieved in the same way as in STED, which uses a depletion laser to drive fluorophores at the periphery of the excitation into a dark state. With saturated depletion, the size of the effective PSF, Δ_{eff}, becomes:

$$\Delta_{eff} \approx \frac{\Delta}{\sqrt{1+I/I_S}}$$

where Δ is the diffraction limited size of the PSF, I is the peak intensity of the depletion laser and I_S is the saturation intensity for the fluorophore. Super resolution can be achieved when the degree of saturation, I / I_S, becomes much larger than unity. Unlike STED which features a high I_S value (~10^7 W/cm^2) and thus requiring an intense depletion laser (often > 10^9 W/cm^2), an optical transition that has low I_S can be chosen for RESOLFT, allowing super-resolution imaging at a much lower depletion laser intensity (3). For example, RESOLFT has been demonstrated using a reversibly photoswitchable fluorescent protein asFP595 which leads to a resolution better than 100 nm at a depletion laser intensity of 600 W/cm^2(30).

Saturated structured illumination microscopy (SSIM)

The same concept of employing saturable processes can also be applied to SIM by introducing sub-diffraction-limit spatial features into the excitation pattern. SSIM has been demonstrated using the saturation of fluorescence emission, which occurs when a fluorophore is illuminated by a very high intensity of excitation light (4). Under this strong excitation, it is immediately pumped to the excited state each time it returns to the ground state, and the fluorescence lifetime becomes the limiting factor for the fluorescent emission rate. Consequently, as the fluorescence intensity of the fluorophore approaches a saturation level, it is no longer proportional to the excitation light intensity. In SSIM, where the sample is illuminated with a sinusoidal pattern of strong excitation light, the peaks of the excitation pattern can be clipped by fluorescence saturation and become flat, whereas fluorescence emission is still absent from the zero points in the valleys (Figure 3a). These effects add higher order spatial frequencies to the excitation pattern. Mixing this excitation pattern with the high-frequency spatial features in the sample can effectively bring the sub-diffraction-limit spatial features into the detection range of the microscopy (Figure 3b). A super-resolution image can then be reconstructed in a similar manner as in SIM. Like STED and RESOLFT, the spatial resolution of SSIM is no longer fundamentally limited by diffraction, but rather by the level of fluorescence saturation than can be practically reached. SSIM has demonstrated a 50-nm resolution in two dimensions (4).

SUPER RESOLUTION FLUORESCENCE MICROSCOPY BY SINGLE-MOLECULE IMAGING

A biological structure is ultimately defined by the positions of the molecules that build up the structure. Similarly, a fluorescence image is defined by the spatial coordinates of the fluorophores that generate the image. It is thus conceivable that super-resolution fluorescence microscopy can also be achieved by determining the position of each fluorescent probe in a sample with high precision.

High-precision localization of single fluorophores

Although the image of a single fluorophore, which resembles the PSF, is a finite-sized spot, the precision of determining the fluorophores position from its image can be much higher than the diffraction limit, as long as the image results from multiple photons emitted from the fluorophore. Fitting an image consisting of N photons can be viewed as N measurements of

the fluorophore position, each with an uncertainty determined by the PSF (8), thus leading to a localization precision approximated by:

$$\Delta_{loc} \approx \frac{\Delta}{\sqrt{N}}$$

where Δ_{loc} is the localization precision and Δ is the size of the PSF. This scaling of the localization precision with the photon number allows super-resolution microscopy with a resolution not limited by the diffraction of light.

High-precision localization of bright light sources, such as fluorescent particles, is often used in biophysical experiments (31,32) and has reached a precision as high as ~1 Å (33). Taking advantage of single-molecule detection and imaging (34,35), nanometer localization precision has also been achieved for single fluorescent molecules under ambient conditions (36). When multiple molecules are present in close proximity, however, localization becomes inaccurate or impossible because the images of these fluorophores overlap. Separation of the fluorescence signal from a few molecules with overlapping images may be achieved in the spectral domain according to their distinct excitation or emission spectra (37–39) or in the time domain, utilizing the fact that different emitters independently undergo photobleaching (40,41) or blinking (42,43). It is, however, difficult to scale up the number of fluorophores that can be resolved within a diffraction-limited area using these methods.

Super resolution fluorescence microscopy using single-molecule localization

A typical fluorescently labeled biological sample, however, contains thousands or even millions of fluorophores at a high density, making them difficult to resolve by the single-molecule localization approach. Using fluorescent probes that can switch between a fluorescent and a dark state, a recent invention overcomes this barrier by separating in the time domain the otherwise spatially overlapping fluorescent images. In this approach, molecules within a diffraction limited region can be activated at different time points so that they can be individually imaged, localized, and subsequently deactivated (Figure 4). Massively parallel localization is achieved through wide-field imaging, so that the coordinates of many fluorophores can be mapped and a super-resolution images subsequently reconstructed. This concept has been independently conceived and implemented by three labs, and it was given the names STORM (5), PALM (6), and FPALM (7), respectively. All three labs initially used photoswitchable fluorescent dyes or proteins that can be activated by light at a wavelength different from the imaging light that excites fluorescence and deactivates the fluorophores. Separating activation and imaging allows one to control the fraction of molecules in the fluorescent state at a given time, such that the activated molecules are optically resolvable from each other and precisely localized. Iterating the activation and imaging process then allows the locationsof many fluorophores to be mapped and a super-resolution image to be constructed from these fluorophore locations. In the following, we refer to this approach as super-resolution microscopy by single-molecule localization. Other variants of this approach have been subsequently reported using asynchronous activation and deactivation of fluorophores (44) or nonoptical processes, such as the stochastic binding of diffusing fluorophores (45).

The photophysical and photochemical properties of fluorescent probes are critical for super-resolution imaging by single-molecule localization. A large number of photoswitchable fluorophores have so far been reported for this application (Table 1). These probes range from organic dyes to FPs, allowing the labeling of biological samples with a variety of methods. The resolution of this technique is limited by the number of photons detected per photoactivation event, which varies from several hundred for FPs (6) to several thousand for cyanine dyes such as Cy5 (5,46). These numbers theoretically allow more than an order of

magnitude improvement in spatial resolution according to the √N scaling rule. In practice, a lateral resolution of ~20 nm has been established experimentally using the photoswitchable cyanine dyes (5,46). Super-resolution images of biological samples have been reported with directly labeled DNA structures and immunostained DNA-protein complexes in vitro (5) as well as with FPtagged or immunostained cellular structures (6,44,46).

RECENT PROGRESSES IN SUPER RESOLUTION FLUORESCENCE MICROSCOPY

Recent advances in super-resolution fluorescence microscopy (including the capability for 3D, multicolor, live-cell imaging) enable new applications in biological samples. These technical advances were made possible through the development of both imaging optics and fluorescent probes.

Three-dimensional (3D) imaging

Most cellular structures are 3D in nature, and the ability to resolve a 3Dstructure is in general limited by the dimension with the lowest resolution. Therefore, it is important to develop techniques that reach super resolution in all three dimensions.

3D imaging using the single-molecule localization approach—Extending the STORM/PALM/FPALM approach to 3D imaging requires determining the 3D position of the activated fluorescent probes. A number of 3D localization methods previously developed for particle tracking (47–51) have been adapted for this purpose.

Super-resolution imaging by single molecule localization was first implemented in three dimensions using the astigmatism method for axial localization (52). This approach inserts a cylindrical lens in the imaging optics so that the image is focused differently in the *x* and *y* directions. Consequently, the image of a single fluorophore becomes elliptical, making it possible to simultaneously measure its axial position from the ellipticity and the lateral position from the centroid of the image. This method has achieved a lateral localization precision of ~25 nm (FWHM) and an axial localization precision of ~50 nm (FWHM) over the depth of several hundred nanometers in z with photoswitchable cyanine dyes (52). Combining with z-scanning allowed whole mammalian cells (several micrometers thick) to be imaged (53). The spatial organization of microtubules in cells, the semispherical shell structure of clathrin-coated pits, with a diameter of about ~150 nm, and the outer membrane structure of mitochondria has been resolved using this technique (52,53) For thick sample imaging, spherical abberations caused by the refractive index mismatch between the sample and the imaging optics also need to be minimized or corrected (53).

Another implementation of 3D superresolution imaging (54) uses two-focal-plane imaging, in which the emission light is split and imaged to two regions of the camera with different path lengths, allowing the determination of z coordinates from the defocused shape of the single-molecule images. This method has achieved 75-nm axial localization precision with caged fluorescein over a depth of several hundred nanometers. Similarly z-scanning further enables the imaging of samples with thicknesses of several micrometers, and 4-μm microspheres were imaged as a demonstration of the technique.

3D imaging using the patterned excitation approach—As discussed above, STED can operate either in the *xy* mode to improve lateral resolution by applying a donut-shaped depletion pattern in the *x*-*y* plane or in the *z* mode to improve the axial resolution by using a depletion pattern with two maxima along the *z* axis. STED can also be employed in 4Pi microscopy (STED-4Pi) to achieve super resolution in *z*. 3D super-resolution imaging requires

a combination of these schemes. For example, super resolution has recently been obtained simultaneously in all three dimensions by applying STED in both *xy* and *z* mode (55) or by combining *xy* STED with STED-4Pi (56). The major obstacle for combining two STED patterns is the interference between the two STED lasers, which can be eliminated either by introducing a time delay between the two STED pulses (55) or by using two independent lasers as the source (56). An isotropic spatial resolution of 40–45 nm has been demonstrated, allowing the observation of the hollow shape of the mitochondrial outer membrane, which has a diameter of 300–500 nm (56).

SSIM has only been demonstrated in two dimensions to date, while the nonsaturated SIM has provided ~100-nm lateral and ~300-nm axial resolution, allowing chromosomes and nuclear envelope structures to be better resolved compared to confocal microscopy (21). It is only natural to expect that SSIM can also be realized for 3D super-resolution imaging by using a structured excitation pattern at the saturation level along both lateral and axial directions.

Multicolor imaging

Resolving a biological structure is important for understanding its functionality, but it is often not sufficient because many biological processes involve interactions between different structures or biomolecules. These interactions are often addressed using multicolor microscopy, wherein different components are labeled with distinctly colored probes. The colocalization between different colors in the image is used as the indicator of possible interactions, but the accuracy of colocalization is inherently limited by the resolution of the imaging method. Multicolor super-resolution imaging thus promises to significantly advance our understanding of molecular interactions in cells.

Multicolor imaging using the patterned excitation approach—Multicolor STED can be performed using fluorophores with different excitation and emission wavelengths. Two-color STED has been realized using two pairs of excitation and STED lasers spanning the blue to NIR range (e.g., excitation at 488 nm and STED at 603 nm for Atto 532; excitation at 635 nm and STED at 750–780 nm for Atto 647N) (57). Another approach is to use dyes with extremely large Stokes shifts, so that two fluorophores can share the same STED laser but can be distinguished according to their different excitation wavelengths. As an example, DY-485XL excited at 488 nm and NK51 excited at 532 nm, both with emissions in the 570–620-nm range and compatible with a 647-nm STED laser, were used for imaging mitochondria outer membrane and matrix in three dimensions (56).

Multicolor imaging using the single-molecule localization approach—The key for multicolor imaging using single-molecule localization is to determine the identity of each activated fluorescent probe. In addition to the excitation and emission wavelength, the activation wavelength can also be used as a fluorophore signature, adding more versatility. The prerequisite for multicolor imaging, therefore, is the availability of photoswitchable probes with distinct excitation, emission, or activation wavelengths. A palette of such probes have been created based on photoswitchable cyanine dyes (46,53,58). Each of these probes consists of a reporter fluorophore, which can switch to a dark state when excited by the imaging light, and an activator fluorophore, which facilitates the activation of the reporter when illuminated by light that matches the activator absorption. Far red or near IR cyanine dyes, such as Cy5, Cy5.5, and Cy7, can function as the photoswitchable reporters, whereas the activator has a wide range of choices among violet- to yellow-absorbing dyes, such as Alexa Fluor 405, Cy2, and Cy3. Combinatorial pairing of the activators and reporters creates many photoswitchable probes that can be distinguished according to their activation or emission wavelengths. Three-color imaging of immobilized DNA molecules, two-color imaging of microtubules and clathrin-coated-pits in cells, and two-color 3D imaging of microtubules and mitochondria have

been demonstrated using these probes by different activation wavelengths (46,53). The Cy5, Cy5.5, and Cy7 dyes can also be spontaneously activated and deactivated by the same imaging laser (23) (for example 647 nm) without the need of activators but emit light of different wavelenths ranging from red to near IR, providing the possibility of multicolor imaging by distinguishing emission color only. More recently, another series of four photochromic rhodamine dyes have also been synthesized, which have the same activation wavelength but different emission wavelengths ranging from green to red. Three-color imaging of fluorescent microspheres and two-color imaging of microtubules and keratin intermediate filaments have been implemented with these probes (59).

Super-resolution imaging using FPs for multicolor imaging is more difficult because most photoswitchable red-emitting FPs have preactivation fluorescence emission that overlaps with the postactivation fluorescence emission of green-emitting FPs. To circumvent the problem, two-color imaging was initially obtained by using a reversibly switching green FP and a red FP that can only be activated once. In this scheme, the green FPs were only imaged after all red FPs were imaged and photobleached (60). In practice, depleting one probe before imaging the other, however, does not allow multicolor imaging of the same region at multiple time points and therefore is not compatible with recording dynamic processes. This problem was overcome by a recently developed Dronpa variant, bsDronpa, with a blue-shifted emission (61), and the dark-to-red switching PAmCherry, which is nonfluorescent prior to photoactivation (62). Pairing bsDronpa with the green-emitting FP Dronpa, or PAmCherry with other FPs having shorter emission wavelengths, allows simultaneous two-color imaging according to their different emission wavelengths, although the the relatively low number of photons emitted by existing short-wavelength FPs tends to limit image resolution severely.

Live cell imaging

The ability to image a live biological sample is one of the advantages of light microscopy. Fluorescence imaging of a live cell has two requirements: specific labeling of the cell and a time resolution that is high enough to record relevant dynamics in the cell. The super-resolution imaging techniques demonstrated to date, including the patterned excitation and single molecule localization approaches, all have a relatively slow imaging speed. The latter approach requires the introduction of photoswitchable probes into live cells, which adds an additional challenge. Nonetheless, many fluorescent proteins and organic dyes, including cyanine dyes (46) and caged dyes, have been shown switchable in live cells. In this section, we describe the recently demonstrated examples of live-cell super-resolution imaging but defer to the next section a discussion of the factors limiting time resolution and the methods developed for live cell labeling.

Live cell imaging using the patterned excitation approach—Because STED has a much smaller PSF than scanning confocal microscopy, STED would inherently take more time to scan though the same size of image field. By increasing the scanning speed and limiting the field of view to a few μm, Westphal and coworkers have observed Brownian motion of a dense suspension of nanoparticles with an impressive rate of 80 frames per second (fps) using STED microscopy (63). More recently, they have demonstrated video-rate (28 fps) imaging of live hippocampal neurons and observed the movement of individual synaptic vesicles with 60–80-nm resolution (64).

Live cell imaging using the single-molecule localization approach—Super-resolution imaging by single-molecule localization is also relatively slow because the final image is in fact a map of fluorophore localizations accumulated over many activation cycles. Sub-diffraction-limit imaging of focal adhesion proteins in live cells has recently been demonstrated (65). Photoswitchable fluorescent protein, EosFP, was used to label the focal

adhesion protein paxillin. A time resolution of ~25–60 seconds per frame was obtained, and during this time interval, approximately 103 fluorophores were activated and localized per square micrometer, providing an effective resolution of 60–70 nm by the Nyquist criterion (65). More recently, super-resolution imaging has also been demonstrated in live bacteria with photoswitchable enhanced yellow fluorescent protein (EYFP), allowing the MreB structure in the cell to be traced (66).

Photoswitchable fluorescent probes can also greatly facilitate particle tracking measurements. Contrary to conventional single-particle tracking experiments, in which only a small fraction of the targets are labeled and tracked, the use of photoswitchable probes allows a high density of target molecules to be labeled. Although only an optically resolvable subset is activated and tracked at a given time, accumulation over many activation cycles allows a high density map of particle tracks to be constructed. This approach has been used to test the existence of membrane microdomains by observing the diffusion and aggregation of hemagglutinin on the plasma membrane (67) and to monitor the spatial map of the diffusion properties of membrane proteins (68).

THE RESOLVABILITY OF SUPER RESOLUTION MICROSCOPY

Microscopy techniques provide the ability to observe both the spatial structure of a specimen and how the specimen changes in time. The spatial and temporal resolution of the technique determine to what degree the fine details of the structure can be observed and how quickly a dynamic process can be followed. This section discusses the limits of resolvability in these aspects of super-resolution fluorescence microscopy and potential ways to overcome these limits.

The optical resolution

Optical resolution is the intrinsic ability of a given method to resolve a structure and can be defined as the ability to distinguish two point sources in proximity. For the patterned excitation approaches, such as STED, SSIM, and RESOLFT, the optical resolution is represented by the size of the effective PSF. For the single-molecule localization approach, such as STORM/PALM/FPALM, the precision of determining the positions of individual fluorescent probes is the principal measure of optical resolution.

The patterned excitation approach—By using a spatially patterned excitation profile, this approach achieve super resolution by generating an effective excitation volume with dimensions far below the diffraction limit. Taking STED as an example, the sharpness of the PSF results from the saturation of depletion of excited-state fluorophores in the region neighboring the zero point of the STED laser (which coincide with the focal point of the excitation laser). With an increasing STED laser power, the saturated region expands toward the zero point, but fluorophores at the zero point are not affected by the STED laser if the zero point is strictly kept at zero intensity. Therefore, a theoretically unlimited gain in spatial resolution may be achieved if the zero point in the depletion pattern is ideal.

In practice, however, nonideal zero points (with finite intensity) can result from many factors, limiting the maximum achievable resolution. For example, a zero point with an intensity that is 1% of the peak intensity would only lead to a factor of ~7 improvement in optical resolution compared to confocal microscopy (according to simulations), whereas a zero point intensity that is 0.1% of the peak intensity could provide a ~20-fold increase in resolution. The zero point intensity of the structured illumination profile has a similar importance in the resolution achievable by SSIM.

Factors leading to nonideal zero points include imperfections in the laser mode, phase plate (for STED) or diffractive grating (for SSIM), and microscope objective, as well as spherical aberrations caused by refractive index mismatch between the coverglass and the medium in which the sample is mounted. In tissue sections where the scattering of light is strong, the gain in optical resolution can be further limited.

Another practical factor that limits resolution is the sample damage by the high laser intensity used for saturated depletion or excitation. The more general approach of RESOLFT microscopy utilizes a light-driven transition between fluorescent and dark states of switchable fluorophores other than stimulated emission to deplete fluorescence emission at the periphery of the zero point. Although it is possible to achieve super resolution at a much lower depletion power with low-saturation-level transitions, the resolution of this technique is more often limited by other factors, including the inability of the depletion laser to completely suppress fluorescence and the number of on-off transition cycles that a fluorescent probe can undergo.

The single-molecule localization approach—The single-molecule localization approach achieves super resolution through high precision localization of individual fluorophores. The number of photons collected from a fluorophore is a principal factor limiting the localization precision and hence the resolution of the final image.

A rigorous way to characterize single molecule localization precision is through repetitive localization of a photoswitchable fluorophore. Alternatively, the localization precision can be obtained from the distribution of measured positions of multiple probes on a well-defined structure, e.g., a flat surface for quantifying the localization precision in *z*. In the example of the photoswitchable cyanine dyes, the localization precision has been characterized experimentally to ~20 nm (FWHM) in the lateral direction (5,46). By contrast, a theoretical resolution of 6 nm (FWHM), or a corresponding standard deviation of 3 nm, would be expected based on 6000 photons detected per activation cycle from these dyes under the specified imaging geometries (8,46). Possible causes for this discrepancy include the facts that the PSF of a fluorophore is not a perfect Gaussian function (L.S. Churchman & J.A. Spudich, personal communication); the image of a nonfreely rotating fluorophore is not symmetric owing to the dipole emission pattern (69); the camera pixels differ slightly in size, quantum efficiency, and gain (S. Chu, personal communication); and residual mechanical instability of the instrument remains after drift correction (5). One must, therefore, be cautious when using the number of detected photons to infer the optical resolution of a particular experiment.

Several photoswitchable fluorophores have been reported to give thousands of photons detected per activation event [e.g., 6000 from Cy5 (46)].With the PSF fitting procedure and the mechanical stability of the system optimized, the background signal suppressed, and the nonuniformity of camera pixels corrected, optical resolution of just a few nanometers could potentially be achieved, reaching the molecular scale. As in the case of the patterned excitation approach, the optical resolution here is also unlimited, in principle, given a sufficient number of photons detected from the fluorescent probes.

Factors affecting the effective spatial resolution

The optical resolution, as discussed above, defines the physical limit of the smallest structure it can resolve. When imaging a biological sample, the effective resolution is also affected by several sample-specific factors, including the labeling density, probe size, and how well the ultrastructures are preserved during sample preparation.

Labeling density—In super-resolution fluorescence microscopy, because the optical resolution often approaches the distance between adjacent fluorescent probes in a sample, the labeling density could become a limiting factor of the effective spatial resolution. This

limitation applies to all super-resolution fluorescence microscopy methods, including STED, RESOLFT, SSIM, as well as STORM/PALM/FPALM. When the labeling efficiency (fraction of target molecules labeled) of a sample is not sufficient, artifacts can be observed in super-resolution images, for example, causing continuous structures to appear discontinuous.

The effect of labeling density on the effective resolution can be quantified by the Nyquist criterion, which states that structural features smaller than twice that of the fluorophore-to-fluorophore distance cannot be reliably discerned (65,70). The smallest resolvable feature size thus follows:

$$\Delta_{\text{Nyquist}}=2/N^{1/D}$$

where N is density of labeling, and D is the dimension of the structure to be imaged. According to this formula, to achieve a 20-nm 2D (or 3D) resolution, an extremely high labeling density of 10^4 per μm^2 (or 10^6 per μm^3) is required in general. In practice, however, a lower requirement on the labeling density is often sufficient when the geometry of the sample is taken into consideration. Biological structures are often so heterogeneous that a high local density can result from a relatively low overall density. For example, when taking a 2D image of clathrin-coated pits, which are~150-nm round structures distributed on the plasma membrane with a surface density of about 0.5 pits per μm^2, an overall labeling density of 90 per μm^2 would already correspond to a local density of 10^4 per μm^2 within individual pits, which is sufficient to obtain a 20-nm lateral resolution.

For the single-molecule localization approach, too high labeling density can also be disadvantageous because the majority of photoswitchable fluorophores are not completely dark in their dark state. They either emit weak fluorescence or can spontaneously switch to the fluorescent state in the absence of activation light. This type of nonspecific activation can either be spontaneous or induced by the imaging laser. Therefore, a large number of nonspecifically activated fluorophores associated with very high labeling density could cause the overlap of single-molecule images, which prevents high-precision localization. In other words, photoswitchable fluorophores with low dark-state emissions and low nonspecific activation rates are desired for ultrahigh-resolution imaging.

Probe size—The size of the probe fundamentally limits on how well the image reflects the actual structure. For example, with indirect immunofluorescence, the binding of the primary and secondary antibodies increases the apparent diameter of microtubules from 25 nm to about 60 nm, which has been observed in both EM (71) and STORM (46). Smaller probes include primary antibodies for direct immunofluorescence (~10–15 nm in size) (52), antibody Fab fragments (~6 nm in size), and FPs (~3–4 nm in size). The ultimate solution of the probe size problem is the direct labeling of target molecules with organic fluorophores (~1 nm).

Immunostaining with dye-labeled antibodies is often the method of choice for tissue imaging because genetic engineering of an animal with FP labels could be time consuming or even impossible (for example, human subjects). Being brighter and more photostable, organic dyes also tend to have more ideal photophysical properties for super-resolution imaging than FPs. For live-cell imaging, a FP is often a more convenient choice because it can be genetically targeted to the molecule of interest inside the cell. The sizes of FPs are also smaller than antibodies. To combine the benefits from both sides, several methods have been recently developed to directly couple an organic dye molecule to a specific protein through genetic coding (72,73). These methods fuse the protein of interest to a specific peptide sequence, which either exhibits direct affinity to certain fluorescence dyes [such as the tetracysteine tag binding to biarsenic fluorophores (74) and the polyhistindine tag binding to the NTA group (75)] or

can be covalently linked to dye molecules through enzymatic reactions [such as those catalyzed by biotin ligase (76), liopoic acid ligase (77), and sortase (78)].

Biomolecules other than proteins can also be fluorescently stained for super-resolution microscopy. Membrane structures can be probed with fluorescent lipids. Glycosylation patterns were detected using fluorescently labeled lectins or through metabolism of synthetic azidosugar (79). Fluorescence in situ hybridization using photoswitchable probes could enable mapping the localization of specific DNA sequences or RNAs in a cell. The further development of methods for efficient and specific labeling of cellular structures with small and bright fluorophores will be highly beneficial for super-resolution fluorescence microscopy.

Preservation of ultrastructures—Damage or alteration to the ultrastructures during sample preparation can lead to artifacts in super-resolution imaging, even though they are not normally apparent in conventional fluorescence microscopy. For immunostaining, suboptimal fixation methods could break molecular structures, and strong permeabilization reagents tend to distort membrane protein distributions. One example of such artifacts is that methanol or formaldehyde fixation, although often used for conventional immunofluorescence, is known to cause significant changes to the ultrastructures of cytoskeletons that are visible in EM. Sample preparation methods developed for EM, such as rapid freezing, freeze-substitution, and fixation with glutaraldehyde (80), could benefit super-resolution fluorescence imaging. For labeling with FPs, the commonly encountered overexpression of the protein tagged with FP can also change the ultrastructures of organelles and distributions of molecules. The side effects of FP tagging and overexpression should thus be carefully controlled in super-resolution imaging.

The time resolution

The time resolution of an imaging technique limits the dynamic information of a biological process that can be extracted through the method. Because of the trade-off between time and spatial resolutions intrinsically involved in all high-resolution imaging approaches, super-resolution fluorescence microscopy is in general slower than conventional fluorescence microscopy under similar instrumental conditions. Here, we provide a brief discussion of the factors limiting the imaging speed of super-resolution microscopy and a comparison of the two super-resolution microscopy approaches in terms of time resolution.

The patterned excitation approach—The most common forms of STED and RESOLFT microscopy are point-scanning techniques similar to scanning confocal microscopy. The higher spatial resolution of STED and RESOLFT, however, implies a smaller scanning pixel size and thus inherently slower acquisition speed when imaging the same sample. The ability to increase the acquisition rate by shortening the dwell time at each scanning pixel is limited by the photon emission rate of the fluorophore and, in the case of RESOLFT, the switching rate of the fluorophore. Therefore, in order to achieve relatively fast time resolution, a reduced area of the image field and an enlarged pixel size are typically used. For example, a 28 frame per second acquisition rate in 2D STED microscopy has been realized for live-cell imaging in a ~2.5 μm × 1.8 μm field of view by using 30-nm pixel size (for 62-nm lateral resolution) (64).

The imaging speed becomes significantly slower for a larger field of view and more so for 3Dimaging. Extrapolating from the parameters given above, the frame rate would be reduced to 0.14 fps when imaging a 30-μm × 30-μm area, which is comparable to the size of a mammalian cell. It will take a further reduction by a factor of 100 when imaging a 3-μm thick sample (roughly the thickness of a surface-adhering cell in culture) in three dimensions, leading to ~12 minutes per frame. The time resolution may be significantly increased by scanning with

multiple excitation focal points, an approach that has been used in the wide-field type of RESOLFT microscopy (81).

The single-molecule localization approach—This approach is intrinsically a wide-field imaging method, and 3D imaging has also been realized without scanning for a relatively thin sample (several hundred nanometers thick) (52). These properties give the single-molecule localization approach advantages when imaging a larger field of view. The imaging speed of this approach is, however, limited by the time required to accumulate a fluorophore localization density that is sufficient for a desired resolution given by the Nyquist criterion, as described earlier. Because different subsets of fluorescent probes are localized sequentially, the time resolution of super-resolution imaging is intrinsically slower than conventional wide-field light microscopy. For example, the observation of the focal adhension morphology, for example, employed a 30 s per frame rate to achieve a ~70-nm Nyquist-limited lateral resolution in a 30 μm × 25 μm field of view (65).

The rate of accumulating localization points is limited by the switching kinetics of fluorescent probes and the acquisition rate of the camera. Photoswitchable fluorophores have been reported to exhibit an off-switching time on the order of 1 ms (82). At this high off-switching/acquisition rate of 1 kHz, probe molecules can be activated at a rate of ~1000 μm^{-2} s^{-1} without causing substantial overlap between single-molecule images, giving a Nyquist-limited lateral resolution of about 60 nm at 1 s time resolution for homogenous structures in a 30 μm × 30 μm region. 3D imaging at 60 nm Nyquist resolution in a 30 μm × 30 μm × 3 μm volume can be performed at about 100 s per frame. As discussed above, for heterogeneous structures, which biological samples usually are, a lower number of localizations is typically needed to achieve the specified resolution, and the imaging speed will be even faster. This projected imaging speed is faster than that of STED for large area imaging, although STED is expected to offer faster imaging for sufficiently small sample areas because the image speed of STORM/PALM/FPALM would not increase as rapidly as STED with reducing image area.

APPLICATIONS IN BIOLOGICAL SYSTEMS

In addition to biomolecular structures prepared in vitro such as DNA and DNA-protein complexes (5), numerous cellular structures have also been imaged using methods described above. Here, we list several examples, which are by no means exhaustive, to demonstrate the capabilities of super-resolution fluorescence microscopy for cell imaging.

The cytoskeleton of mammalian cells, especially microtubules (Figure 5a) (29, 44, 46, 52), is the most commonly used benchmark structure for super-resolution imaging. Other cytoskeletal structures imaged so far include actin filaments in the lamellipodium (6), keratin intermediate filaments (59), neurofilaments (26, 83) and MreB in Caulobacter (66). These images have shown the ability of super-resolution fluorescence microscopy to separate nearby filaments and overlapped and unresolvable in conventional fluorescence images (46, 52), as well as to reveal the 3D organization of the cytoskeleton in a mammalian cell (52).

Organelles, such as the endoplasmic reticulum (27), lysosome (6), endocytic and exocytic vesicles (46,52,64), and mitochondria (6,53,56), have also been imaged. For example, using the single-molecule localization approach, 3D STORM imaging has clearly resolved the ~150-nm diameter, hemispherical cage shape of clathrin-coated pits (46,52), which only appear as diffraction-limited spots without any feature in conventional fluorescence microscopy (Figure 5a,b).Two-color 3D STED has resolved the hollow shape of the mitochondrial outer membrane (marked by the translocase protein Tom20), enclosing a matrix protein Hsp60 (56), even though the diameter of mitochondria is only about 300–500 nm (Figure 5c). The outer membrane structure of mitochondria and their interactions with microtubules have been resolved by two-

color 3D STORM (53). The transport of synaptic vesicles has been recorded at video rate using 2D STED (Figure 5d) (64).

Many plasma membrane proteins or membrane associated protein complexes have also been studied by super-resolution fluorescence microscopy. For example, synaptotagmin clusters after exocytosis in primary cultured hippocampal neurons (84), the donut-shaped clusters of Drosophila protein Bruchpilot at the neuromuscular synaptic active zone (85), and the size distribution of syntaxin clusters have all been imaged (86,87). Photoactivation has enabled the tracking of the influenza protein hemagglutinin and the retroviral protein Gag in live cells, revealing the membrane microdomains (67) and the spatial heterogeneity of membrane diffusion (68). The morphology and transport of the focal adhension complex has also been observed using live-cell PALM (Figure 5e) (65).

The many different types of cellular structures imaged to date with various superresolution fluorescence microscopy techniques demonstrate the power and versatility of these methods.

CONCLUDING REMARKS

Although still in its infancy, super-resolution fluorescence microscopy has shown great promise in studying biological structures and processes at the cellular to macromolecular scale. The rapid pace of development of all forms of super-resolution imaging techniques in recent years is expected to spur further development of novel fluorescent probes and new labeling methods as well as to extend the availability of such techniques to the wider research community. Images obtained from these new super-resolution approaches will enable scientists to directly visualize biological samples at the nanometer scale and will complement the insights obtained through traditional molecular and cell biology approaches, significantly expanding our understanding of molecular interactions and dynamic processes in living systems.

Summary points

1. Super resolution fluorescence microscopy with a spatial resolution not limited by the diffraction of light has been implemented using saturated depletion/excitation or single-molecule localization of switchable fluorophores.
2. Three-dimensional imaging with an optical resolution as high as ~20 nm in the lateral direction and 40–50 nm in axial dimension has been achieved.
3. The resolution of these super-resolution fluorescence microscopy techniques can in principle reach molecular scale.
4. In practice, the resolution of the images are not only limited by the intrinsic optical resolution, but also by sample specific factors including the labeling density, probe size and sample preservation.
5. Multicolor super resolution imaging has been implemented, allowing colocalization measurements to be performed at nanometer scale resolution and molecular interaction to be more précised identified in cells.
6. Super-resolution fluorescence imaging allows dynamic processes to be investigated at the tens of nanometer resolution in living cells.
7. Many cellular structures have been imaged at sub-diffraction-limit resolution.

Future issues

1. Achieving molecular scale resolution (a few nanometers or less).

2. Fast super resolution imaging of a large view field by multi-point scanning or high-speed single-molecule switching/localization.
3. Developing new fluorescent probes that are brighter, more photostable and switchable fluorophores that have high on-off contrast and fast switching rate.
4. Developing fluorescent labeling methods that can stain the target with small molecules at high specificity, high density and good ultrastructure preservation.
5. Application of super resolution microscopy to provide novel biological insights

Acronyms

FP	Fluorescent Protein
FPALM	Fluorescence PhotoActivation Localization Microscopy
I^5M	Combination of I^2M (Illumination Interference Microscopy) and I^3M (Incoherent Imaging Interference Microscopy)
PALM	PhotoActivated Localization Microscopy
PSF	Point Spread Function
RESOLFT	REversible Saturable Optically Linear Fluorescence Transition
SIM	Structured Illumination Microscopy
SSIM	Saturated Structured Illumination Microscopy
STED	STimulated Emission Depletion
STORM	STochastic Optical Reconstruction Microscopy

glossary

Numerical aperture (NA)	The numerical aperture of an objective characterizes the solid angle of light collected from a point light source at the focus of the objective.
Stimulated emission	The process that an excited state molecule or atom jumps to the ground state by emitting another photon that is identical to the incoming photon. It is the basis of laser.
Fluorescence saturation	At high excitation intensity, the fluorescence lifetime instead of the excitation rate becomes the rate limiting step of fluorescence emission, causing the fluorescence signal not to increase proportionally with the excitation intensity.
Nyquist criterion	To determine a structure, the sampling interval needs to be no larger than half of the feature size.
Mitochondria	Organelles in eukaryotic cells for APT generation, consisting of two membrane (inner and outer) enclosing the inter membrane space and the matrix inside the inner membrane.
Clathrin-coated pit	Vesicle forming machinery involved in endocytosis and intracellular vesicle transport, consisting of clathrin coats, adapter proteins, and other regulatory proteins.

Focal adhesion	The macromolecular complex serving as the mechanical connection and signaling hub between a cell and the extracellular matrix or other cells.

Acknowledgments

This work is supported by in part by the National Institute of Health (to X.Z.). X.Z. is a Howard Hughes Medical Institute Investigator.

References

1. Hell SW, Wichmann J. Breaking the diffraction resolution limit by stimulated-emission: stimulated emission- depletion fluorescence microscopy. Opt. Lett 1994;19:780–782. [PubMed: 19844443]
2. Klar TA, Hell SW. Subdiffraction resolution in far-field fluorescence microscopy. Opt. Lett 1999;24:954–956. [PubMed: 18073907]
3. Hell SW. Far-field optical nanoscopy. Science 2007;316:1153–1158. [PubMed: 17525330]
4. Gustafsson MGL. Nonlinear structured-illumination microscopy: wide-field fluorescence imaging with theoretically unlimited resolution. Proc. Natl. Acad. Sci. USA 2005;102:13081–13086. [PubMed: 16141335]
5. Rust MJ, Bates M, Zhuang X. Sub-diffraction-limit imaging by stochastic optical reconstruction microscopy (STORM). Nat. Methods 2006;3:793–795. [PubMed: 16896339]
6. Betzig E, Patterson GH, Sougrat R, Lindwasser OW, Olenych S, et al. Imaging intracellular fluorescent proteins at nanometer resolution. Science 2006;313:1642–1645. [PubMed: 16902090]
7. Hess ST, Girirajan TPK, Mason MD. Ultra-high resolution imaging by fluorescence photoactivation localization microscopy. Biophys. J 2006;91:4258–4272. [PubMed: 16980368]
8. Thompson RE, Larson DR, Webb WW. Precise nanometer localization analysis for individual fluorescent probes. Biophys. J 2002;82:2775–2783. [PubMed: 11964263]
9. Pohl DW, Denk W, Lanz M. Optical stethoscopy: image recording with resolution lambda/20. Appl. Phys. Lett 1984;44:651–653.
10. Betzig E, Trautman JK, Harris TD, Weiner JS, Kostelak RL. Breaking the diffraction barrier: optical microscopy on a nanometric scale. Science 1991;251:1468–1470. [PubMed: 17779440]
11. Novotny, L.; Hecht, B. Principles of Nano-Optics. Cambridge: Cambridge Univ. Press; 2006.
12. Smolyaninov II, Hung YJ, Davis CC. Magnifying superlens in the visible frequency range. Science 2007;315:1699–1701. [PubMed: 17379804]
13. Liu ZW, Lee H, Xiong Y, Sun C, Zhang X. Far-field optical hyperlens magnifying subdiffractionlimited objects. Science 2007;315:1686. [PubMed: 17379801]
14. Pawley, JB., editor. Handbook of Biological Confocal Microscopy. New York: Springer; 2006.
15. Zipfel WR, Williams RM, Webb WW. Nonlinear magic: multiphoton microscopy in the biosciences. Nat. Biotechnol 2003;21:1368–1376.
16. Hell S, Stelzer EHK. Fundamental improvement of resolution with a 4Pi-confocal fluorescence microscope using two-photon excitation. Opt. Comm 1992;93:277–282.
17. Gustafsson MGL, Agard DA, Sedat JW. I5M: 3D widefield light microscopy with better than 100 nm axial resolution. J. Microsc 1999;195:10–16. [PubMed: 10444297]
18. Bailey B, Farkas DL, Taylor DL, Lanni F. Enhancement of axial resolution in fluorescence microscopy by standing-wave excitation. Nature 1993;366:44–48. [PubMed: 8232536]
19. Gustafsson MGL. Surpassing the lateral resolution limit by a factor of two using structured illumination microscopy. J. Microsc 2000;198:82–87. [PubMed: 10810003]
20. Gustafsson MGL, Shao L, Carlton PM, Wang CJR, Golubovskaya IN, et al. Three-dimensional resolution doubling in wide-field fluorescence microscopy by structured illumination. Biophys. J 2008;94:4957–4970. [PubMed: 18326650]

21. Schermelleh L, Carlton PM, Haase S, Shao L, Winoto L, et al. Subdiffraction multicolor imaging of the nuclear periphery with 3D structured illumination microscopy. Science 2008;320:1332–1336. [PubMed: 18535242]
22. Shao L, Isaac B, Uzawa S, Agard DA, Sedat JW, Gustafsson MGL. I5S:Wide-field light microscopy with 100-nm-scale resolution in three dimensions. Biophys. J 2008;94:4971–4983. [PubMed: 18326649]
23. Heilemann M, van de Linde S, Sch¨uttpelz M, Kasper R, Seefeldt B, et al. Subdiffraction-resolution fluorescence imaging with conventional fluorescent probes. Angew. Chem. Int. Ed. Engl 2008;47:6172–6176. [PubMed: 18646237]
24. Westphal V, Hell SW. Nanoscale resolution in the focal plane of an optical microscope. Phys. Rev. Lett 2005;94:143093.
25. Dyba M, Hell SW. Focal spots of size lambda/23 open up far-field florescence microscopy at 33 nm axial resolution. Phys. Rev. Lett 2002;88:163901. [PubMed: 11955234]
26. Donnert G, Keller J, Medda R, Andrei MA, Rizzoli SO, et al. Macromolecular-scale resolution in biological fluorescence microscopy. Proc. Natl. Acad. Sci. USA 2006;103:11440–11445. [PubMed: 16864773]
27. Willig KI, Kellner RR, Medda R, Hein B, Jakobs S, Hell SW. Nanoscale resolution in GFP-based microscopy. Nat. Methods 2006;3:721–723. [PubMed: 16896340]
28. Hell SW, Kroug M. Ground-state-depletion fluorescence microscopy: a concept for breaking the diffraction resolution limit. Appl. Phys. B 1995;60:495–497.
29. Bretschneider S, Eggeling C, Hell SW. Breaking the diffraction barrier in fluorescence microscopy by optical shelving. Phys. Rev. Lett 2007;98:218103. [PubMed: 17677813]
30. Hofmann M, Eggeling C, Jakobs S, Hell SW. Breaking the diffraction barrier in fluorescence microscopy at low light intensities by using reversibly photoswitchable proteins. Proc. Natl. Acad. Sci. USA 2005;102:17565–17569. [PubMed: 16314572]
31. Gelles J, Schnapp BJ, Sheetz MP. Tracking kinesin-driven movements with nanometre-scale precision. Nature 1988;331:450–453. [PubMed: 3123999]
32. Ghosh RN, Webb WW. Automated detection and tracking of individual and clustered cell-surface low-density-lipoprotein receptor molecules. Biophys. J 1994;66:1301–1318. [PubMed: 8061186]
33. Abbondanzieri EA, Greenleaf WJ, Shaevitz JW, Landick R, Block SM. Direct observation of basepair stepping by RNA polymerase. Nature 2005;438:460–465. [PubMed: 16284617]
34. Moerner WE, Kador L. Optical-detection and spectroscopy of single molecules in a solid. Phys. Rev. Lett 1989;62:2535–2538. [PubMed: 10040013]
35. Orrit M, Bernard J. Single pentacene molecules detected by fluorescence excitation in a paraterphenyl crystal. Phys. Rev. Lett 1990;65:2716–2719. [PubMed: 10042674]
36. Yildiz A, Forkey JN, McKinney SA, Ha T, Goldman YE, Selvin PR. MyosinVwalks hand-overhand: single fluorophore imaging with 1.5-nm localization. Science 2003;300:2061–2065. [PubMed: 12791999]
37. van Oijen AM, Kohler J, Schmidt J, Muller M, Brakenhoff GJ. 3-Dimensional super-resolution by spectrally selective imaging. Chem. Phys. Lett 1998;292:183–187.
38. Lacoste TD, Michalet X, Pinaud F, Chemla DS, Alivisatos AP, Weiss S. Ultrahigh-resolution multicolor colocalization of single fluorescent probes. Proc. Natl. Acad. Sci. USA 2000;97:9461–9466. [PubMed: 10931959]
39. Churchman LS, Okten Z, Rock RS, Dawson JF, Spudich JA. Single molecule high-resolution colocalization of Cy3 and Cy5 attached to macromolecules measures intramolecular distances through time. Proc. Natl. Acad. Sci. USA 2005;102:1419–1423. [PubMed: 15668396]
40. Gordon MP, Ha T, Selvin PR. Single-molecule high-resolution imaging with photobleaching. Proc. Natl. Acad. Sci. USA 2004;101:6462–6465. [PubMed: 15096603]
41. Qu XH, Wu D, Mets L, Scherer NF. Nanometer-localized multiple single-molecule fluorescence microscopy. Proc. Natl. Acad. Sci. USA 2004;101:11298–11303. [PubMed: 15277661]
42. Lidke KA, Rieger B, Jovin TM, Heintzmann R. Superresolution by localization of quantum dots using blinking statistics. Opt. Express 2005;13:7052–7062. [PubMed: 19498727]

43. Lagerholm BC, Averett L, Weinreb GE, Jacobson K, Thompson NL. Analysis method for measuring submicroscopic distances with blinking quantum dots. Biophys. J 2006;91:3050–3060. [PubMed: 16861265]
44. Egner A, Geisler C, von Middendorff C, Bock H, Wenzel D, et al. Fluorescence nanoscopy in whole cells by asynchronous localization of photoswitching emitters. Biophys. J 2007;93:3285–3290. [PubMed: 17660318]
45. Sharonov A, Hochstrasser RM. Wide-field subdiffraction imaging by accumulated binding of diffusing probes. Proc. Natl. Acad. Sci. USA 2006;103:18911–18916. [PubMed: 17142314]
46. Bates M, Huang B, Dempsey GT, Zhuang X. Multicolor super-resolution imaging with photoswitchable fluorescent probes. Science 2007;317:1749–1753. [PubMed: 17702910]
47. Kao HP, Verkman AS. Tracking of single fluorescent particles in 3 dimensions: use of cylindrical optics to encode particle position. Biophys. J 1994;67:1291–1300. [PubMed: 7811944]
48. Schutz GJ, Pastushenko VP, Gruber HJ, Knaus H-G, Pragl B, Schindler H. 3Dimaging of individual ion channels in live cells at 40 nm resolution. Single Mol 2000;1:25–31.
49. Holtzer L, Meckel T, Schmidt T. Nanometric three-dimensional tracking of individual quantum dots in cells. Appl. Phys. Lett 2007;90 053902.
50. Toprak E, Balci H, Blehm BH, Selvin PR. Three-dimensional particle tracking via bifocal imaging. Nano Lett 2007;7:2043–2045. [PubMed: 17583964]
51. Watanabe TM, Sato T, Gonda K, Higuchi H. Three-dimensional nanometry of vesicle transport in living cells using dual-focus imaging optics. Biochem. Biophys. Res. Commun 2007;359:1–7. [PubMed: 17512495]
52. Huang B, Wang W, Bates M, Zhuang X. Three-dimensional super-resolution imaging by stochastic optical reconstruction microscopy. Science 2008;319:810–813. [PubMed: 18174397]
53. Huang B, Jones SA, Brandenburg B, Zhuang X. Whole-cell 3D STORM reveals interactions between cellular structures with nanometer-scale resolution. Nat. Methods 2008;5:1047–1052. [PubMed: 19029906]
54. Juette MF, Gould TJ, Lessard MD, Mlodzianoski MJ, Nagpure BS, et al. Three-dimensional sub-100 nm resolution fluorescence microscopy of thick samples. Nat. Methods 2008;5:527–529. [PubMed: 18469823]
55. Harke B, Ullal CK, Keller J, Hell SW. Three-dimensional nanoscopy of colloidal crystals. Nano Lett 2008;8:1309–1313. [PubMed: 18166070]
56. Schmidt R, Wurm CA, Jakobs S, Engelhardt J, Egner A, Hell SW. Spherical nanosized focal spot unravels the interior of cells. Nat. Methods 2008;5:539–544. [PubMed: 18488034]
57. Donnert G, Keller J, Wurm CA, Rizzoli SO, Westphal V, et al. Two-color far-field fluorescence nanoscopy. Biophys. J 2007;92:L67–L69. [PubMed: 17307826]
58. Bates M, Blosser TR, Zhuang XW. Short-range spectroscopic ruler based on a single-molecule optical switch. Phys. Rev. Lett 2005;94:108101. [PubMed: 15783528]
59. Bossi M, F¨olling J, Belov VN, Boyarskiy VP, Medda R, et al. Multicolor far-field fluorescence nanoscopy through isolated detection of distinct molecular species. Nano Lett 2008;8:2463–2468. [PubMed: 18642961]
60. Shroff H, Galbraith CG, Galbraith JA, White H, Gillette J, et al. Dual-color superresolution imaging of genetically expressed probes within individual adhesion complexes. Proc. Natl. Acad. Sci. USA 2007;104:20308–20313. [PubMed: 18077327]
61. Andresen M, Stiel AC, Fölling J, Wenzel D, Schönle A, et al. Photoswitchable fluorescent proteins enable monochromatic multilabel imaging and dual color fluorescence nanoscopy. Nat. Biotechnol 2008;26:1035–1040. [PubMed: 18724362]
62. Subach FV, Patterson GH, Manley S, Gillette JM, Lippincott-Schwartz J, Verkhusha VV. Photoactivatable mCherry for high-resolution two-color fluorescence microscopy. Nat. Methods 2009;6:153–159. [PubMed: 19169259]
63. Westphal V, Lauterbach MA, Di Nicola A, Hell SW. Dynamic far-field fluorescence nanoscopy. New J. Phys 2007;9:10.
64. Westphal V, Rizzoli SO, Lauterbach MA, Kamin D, Jahn R, Hell SW. Video-rate far-field optical nanoscopy dissects synaptic vesicle movement. Science 2008;320:246–249. [PubMed: 18292304]

65. Shroff H, Galbraith CG, Galbraith JA, Betzig E. Live-cell photoactivated localization microscopy of nanoscale adhesion dynamics. Nat. Methods 2008;5:417–423. [PubMed: 18408726]
66. Biteen JS, Thompson MA, Tselentis NK, Bowman GR, Shapiro L, Moerner WE. Super-resolution imaging in live *Caulobacter crescentus* cells using photoswitchable EYFP. Nat. Methods 2008;5:947–949. [PubMed: 18794860]
67. Hess ST, Gould TJ, Gudheti MV, Maas SA, Mills KD, Zimmerberg J. Dynamic clustered distribution of hemagglutinin resolved at 40 nm in living cell membranes discriminates between raft theories. Proc. Natl. Acad. Sci. USA 2007;104:17370–17375. [PubMed: 17959773]
68. Manley S, Gillette JM, Patterson GH, Shroff H, Hess HF, et al. High-density mapping of singlemolecule trajectories with photoactivated localization microscopy. Nat. Methods 2008;5:155–157. [PubMed: 18193054]
69. Enderlein J, Toprak E, Selvin PR. Polarization effect on position accuracy of fluorophore localization. Opt. Express 2006;14:8111–8120. [PubMed: 19529183]
70. Shannon CE. Communication in the presence of noise. Proc. Inst. Radio Eng 1949;37:10–21.
71. Weber K, Rathke PC, Osborn M. Cytoplasmic microtubular images in glutaraldehyde-fixed tissueculture cells by electron-microscopy and by immunofluorescence microscopy. Proc. Natl. Acad. Sci. USA 1978;75:1820–1824. [PubMed: 417343]
72. Chen I, Ting AY. Site-specific labeling of proteins with small molecules in live cells. Curr. Opin. Biotechnol 2005;16:35–40. [PubMed: 15722013]
73. Lin MZ, Wang L. Selective labeling of proteins with chemical probes in living cells. Physiology 2008;23:131–141. [PubMed: 18556466]
74. Griffin BA, Adams SR, Tsien RY. Specific covalent labeling of recombinant protein molecules inside live cells. Science 1998;281:269–272. [PubMed: 9657724]
75. Guignet EG, Hovius R, Vogel H. Reversible site-selective labeling of membrane proteins in live cells. Nat. Biotechnol 2004;22:440–444. [PubMed: 15034592]
76. Chen I, Howarth M, Lin WY, Ting AY. Site-specific labeling of cell surface proteins with biophysical probes using biotin ligase. Nat. Methods 2005;2:99–104. [PubMed: 15782206]
77. Fernandez-Suarez M, Baruah H, Martinez-Hernandez L, Xie KT, Baskin JM, et al. Redirecting lipoic acid ligase for cell surface protein labeling with small-molecule probes. Nat. Biotechnol 2007;25:1483–1487. [PubMed: 18059260]
78. Popp MW, Antos JM, Grotenbreg GM, Spooner E, Ploegh HL. Sortagging: a versatile method for protein labeling. Nat. Chem. Biol 2007;3:707–708. [PubMed: 17891153]
79. Saxon E, Bertozzi CR. Cell surface engineering by a modified Staudinger reaction. Science 2000;287:2007–2010. [PubMed: 10720325]
80. McIntosh, JR., editor. Cellular Electron Microscopy. Vol. Vol.79. New York: Academic; 2007.
81. Schwentker MA, Bock H, Hofmann M, Jakobs S, Bewersdorf J, et al. Wide-field subdiffraction RESOLFT microscopy using fluorescent protein photoswitching. Microsc. Res. Tech 2007;70:269–280. [PubMed: 17262791]
82. Geisler C, Sch¨onle A, von Middendorff C, Bock H, Eggeling C, et al. Resolution of lambda/10 in fluorescence microscopy using fast single molecule photo-switching. Appl. Phys. A 2007;88:223–226.
83. Willig KI, Harke B, Medda R, Hell SW. STED microscopy with continuous wave beams. Nat. Methods 2007;4:915–918. [PubMed: 17952088]
84. Willig KI, Rizzoli SO, Westphal V, Jahn R, Hell SW. STED microscopy reveals that synaptotagmin remains clustered after synaptic vesicle exocytosis. Nature 2006;440:935–939. [PubMed: 16612384]
85. Kittel RJ, Wichmann C, Rasse TM, Fouquet W, Schmidt M, et al. Bruchpilot promotes active zone assembly, Ca2+ channel clustering, and vesicle release. Science 2006;312:1051–1054. [PubMed: 16614170]
86. Sieber JJ, Willig KI, Heintzmann R, Hell SW, Lang T. The SNARE motif is essential for the formation of syntaxin clusters in the plasma membrane. Biophys. J 2006;90:2843–2851. [PubMed: 16443657]
87. Sieber JJ, Willig KI, Kutzner C, Gerding-Reimers C, Harke B, et al. Anatomy and dynamics of a supramolecular membrane protein cluster. Science 2007;317:1072–1076. [PubMed: 17717182]

88. Patterson GH, Lippincott-Schwartz J. A photoactivatable GFP for selective photolabeling of proteins and cells. Science 2002;297:1873–1877. [PubMed: 12228718]

89. Chudakov DM, Verkhusha VV, Staroverov DB, Souslova EA, Lukyanov S, Lukyanov KA. Photoswitchable cyan fluorescent protein for protein tracking. Nat. Biotechnol 2004;22:1435–1439. [PubMed: 15502815]

90. Ando R, Hama H, Yamamoto-Hino M, Mizuno H, Miyawaki A. An optical marker based on the UV-induced green-to-red photoconversion of a fluorescent protein. Proc. Natl. Acad. Sci. USA 2002;99:12651–12656. [PubMed: 12271129]

91. Wiedenmann J, Ivanchenko S, Oswald F, Schmitt F, Rocker C, et al. EosFP, a fluorescent marker protein with UV-inducible green-to-red fluorescence conversion. Proc. Natl. Acad. Sci. USA 2004;101:15905–15910. [PubMed: 15505211]

92. Gurskaya NG, Verkhusha VV, Shcheglov AS, Staroverov DB, Chepurnykh TV, et al. Engineering of a monomeric green-to-red photoactivatable fluorescent protein induced by blue light. Nat. Biotechnol 2006;24:461–465. [PubMed: 16550175]

93. Ando R, Mizuno H, Miyawaki A. Regulated fast nucleocytoplasmic shuttling observed by reversible protein highlighting. Science 2004;306:1370–1373. [PubMed: 15550670]

94. Flors C, Hotta J-I, Hiroshi U-I, Dedecker P, Ando R, et al. A stroboscopic approach for fast photoactivation-localization microscopy with Dronpa mutants. J. Am. Chem. Soc 2007;129:13970–13977. [PubMed: 17956094]

95. Stiel AC, Trowitzsch S, Weber G, Andresen M, Eggeling C, et al. 1.8 angstrom bright-state structure of the reversibly switchable fluorescent protein Dronpa guides the generation of fast switching variants. Biochem. J 2007;402:35–42. [PubMed: 17117927]

96. F¨olling J, Belov V, Kunetsky R, Medda R, Schönle A, et al. Photochromic rhodamines provide nanoscopy with optical sectioning. Angew. Chem. Int. Ed 2007;46:6266–6270.

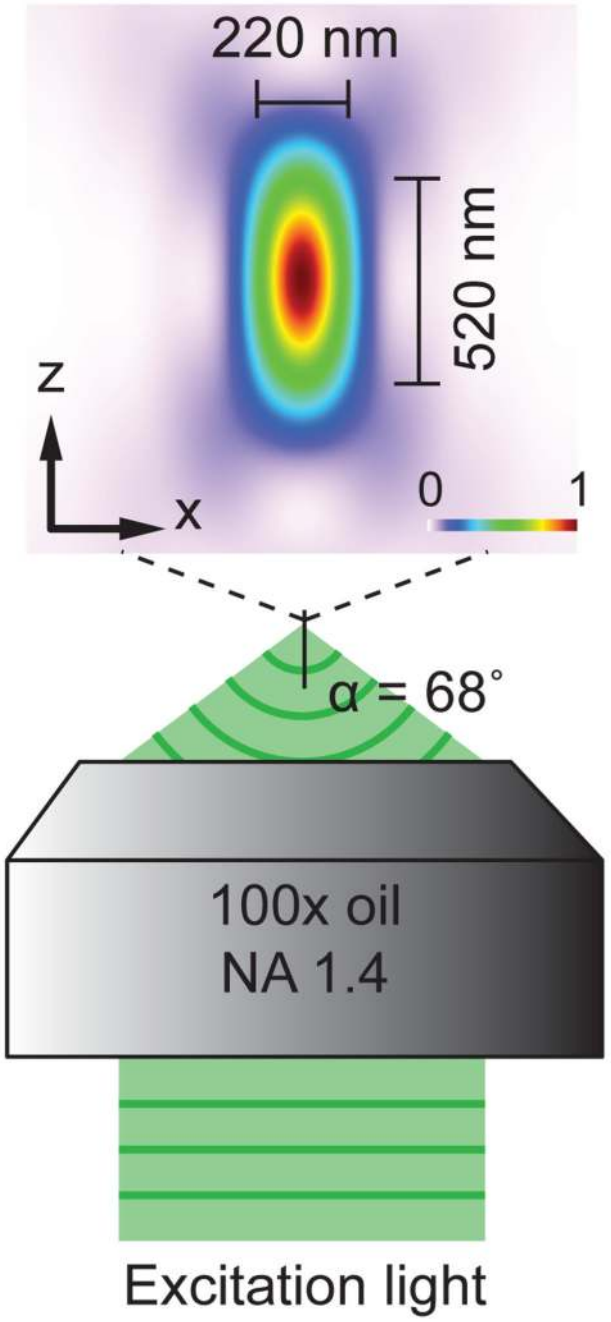

Figure 1.
The PSF of a common oil immersion objective with NA = 1.40, showing the focal spot of 550 nm light in a medium with refractive index $n = 1.515$. The intensity distribution in the x-z plane of the focus spot is computed numerically and shown in the upper panel and the FWHM in the lateral and axial directions are 220 nm and 520 nm, respectively.

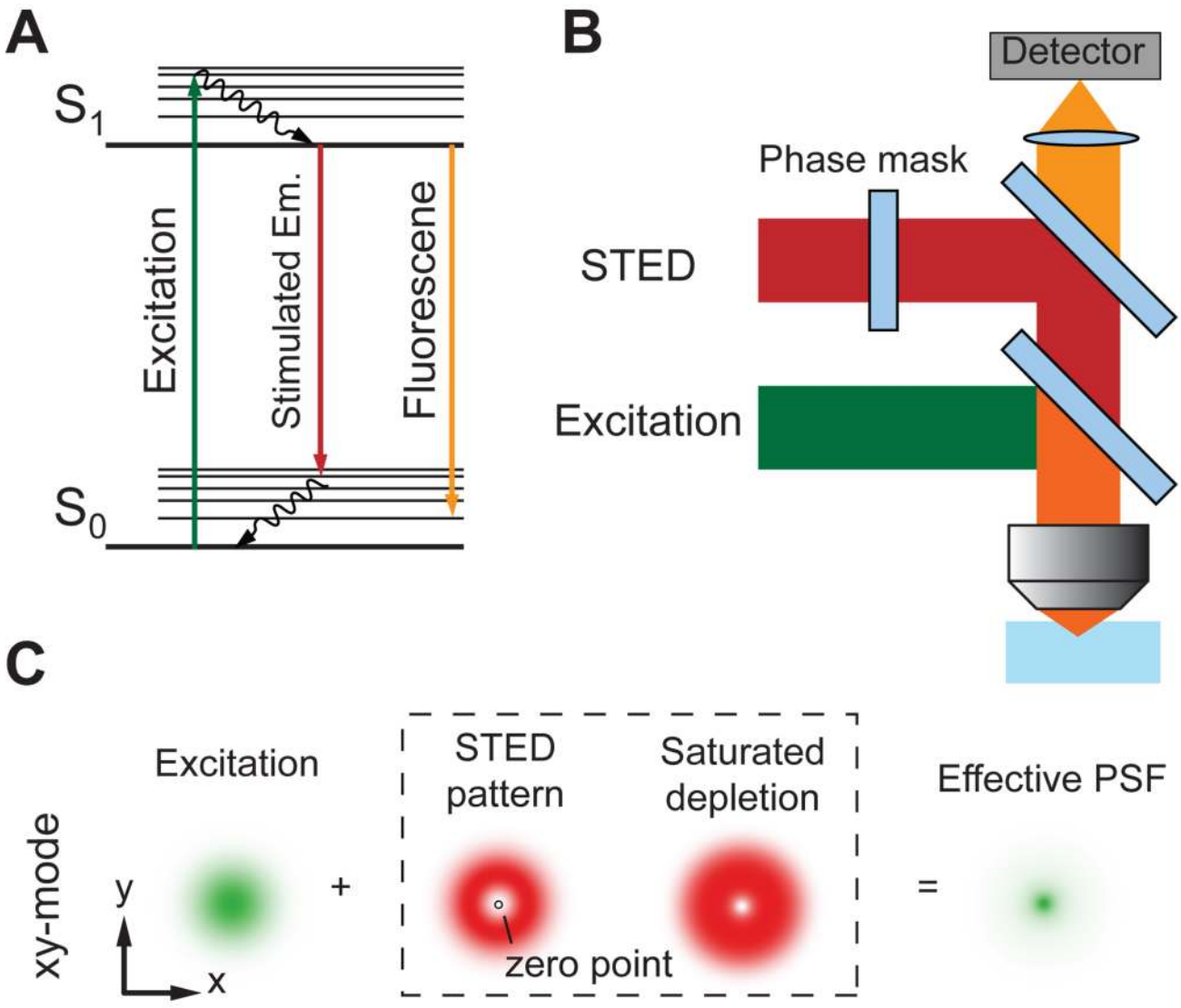

Figure 2.

The principle of STED microscopy. (*a*) The process of stimulated emission. A ground state (S_0) fluorophore can absorb a photon from the excitation light and jump to the excited state (S_1). Spontaneous fluorescence emissionbrings the fluorophore back to the ground state. Stimulated emission happens when the excited state fluorophore encounters another photon with wavelength comparable to the energy difference between the ground and excited state. (*b*) Schematic drawing of a STED microscope. The excitation laser and STED laser are combined and focused into the sample through the objective. A phase mask is placed in the light path of the STED laser to create a specific pattern at the objective focal point. (*c*) In the *xy* mode, a donut-shaped STED laser is applied with the zero point overlapped with the maximum of the excitation laser focus. With saturated depletion, fluorescence from regions near the zero point is suppressed, leading to a decreased size of the effective PSF.

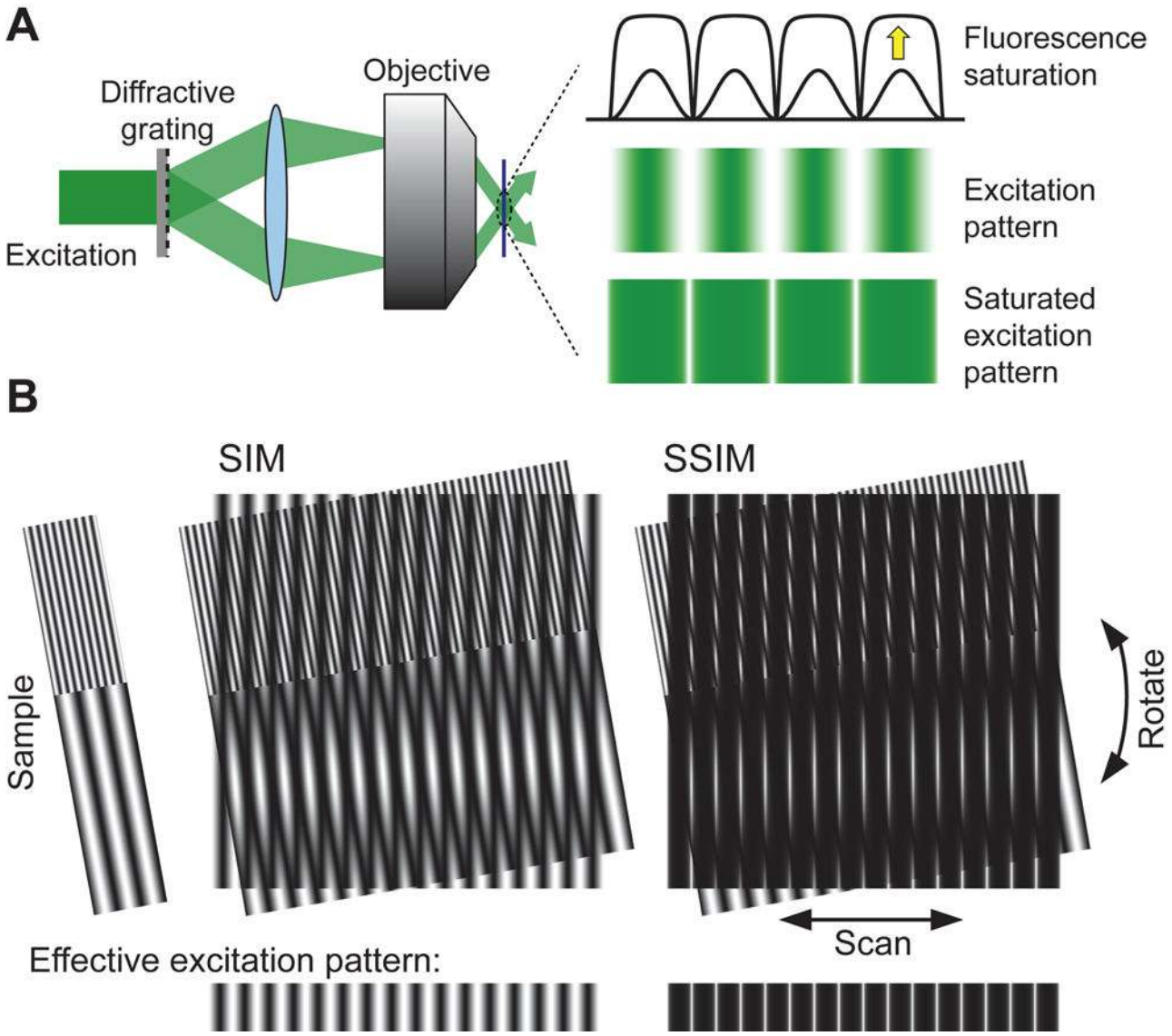

Figure 3.

The principle of SSIM. (*a*) The generation of the illumination pattern. A diffractive grating in the excitation path splits the light into two beams. Their interference after emerging from the objective and reaching the sample creates a sinusoidal illumination pattern with alternating peaks and zero points. Strong excitation light saturates the fluorescence emission at the peaks without exciting fluorophores at the zero points, leading to sharp dark regions in the effective illumination pattern. (*b*) Resolving fine structures with SIM and SSIM. When apply a sinusoidal illumination pattern to a sample, moiré pattern at a significantly lower spatial frequency than that of the sample can be generated and imaged by the microscope (SIM panel, *lower part*). Multiple images resulted from scanning and rotating the excitation pattern are then used to reconstruct the sample structure. However, fine structures with spatial frequencies much higher than the illumination pattern are still indiscernible, as mixing the two does not generate significantly lower spatial frequency in the moiré pattern (SIM panel, *upper part*). SSIM introduces high frequency component into the illumination pattern, allowing features far below the diffraction limit to be resolved (as is evident by the appearance of low frequency moiré pattern in the upper part of the SSIM panel).

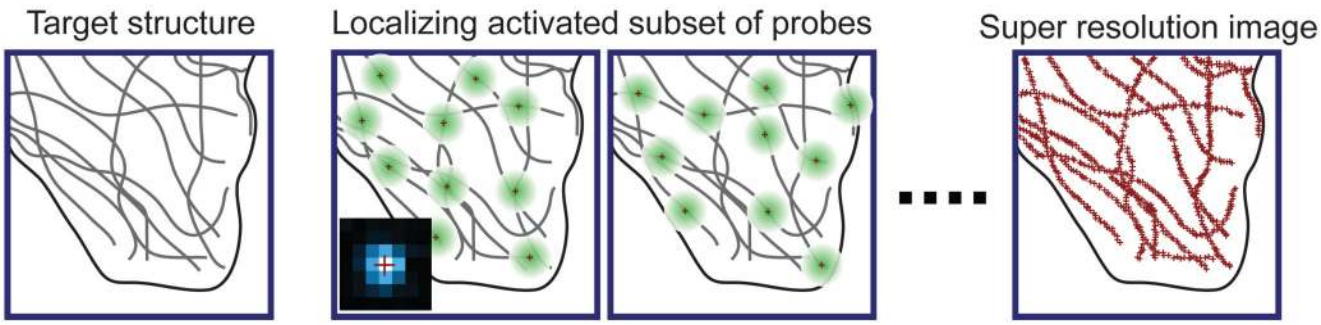

Figure 4.
The principle of stochastic optical reconstruction microscopy (STORM), photoactivated localization microscopy (PALM), and fluorescence photoactivation localization microscopy (FPALM). Different fluorescent probes marking the sample structure are activated at different time points, allowing subsets of fluorophores to be imaged without spatial overlap and to be localized to high precision. Iterating the activation and imaging process allows the position of many fluorescent probes to be determined and a super-resolution image is then reconstructed from the positions of a large number of localized probe molecules. The lower left inset of the second panel shows an experimental image of a single fluorescent dye (*blue*) and the high-precision localization of the molecule (*red cross*).

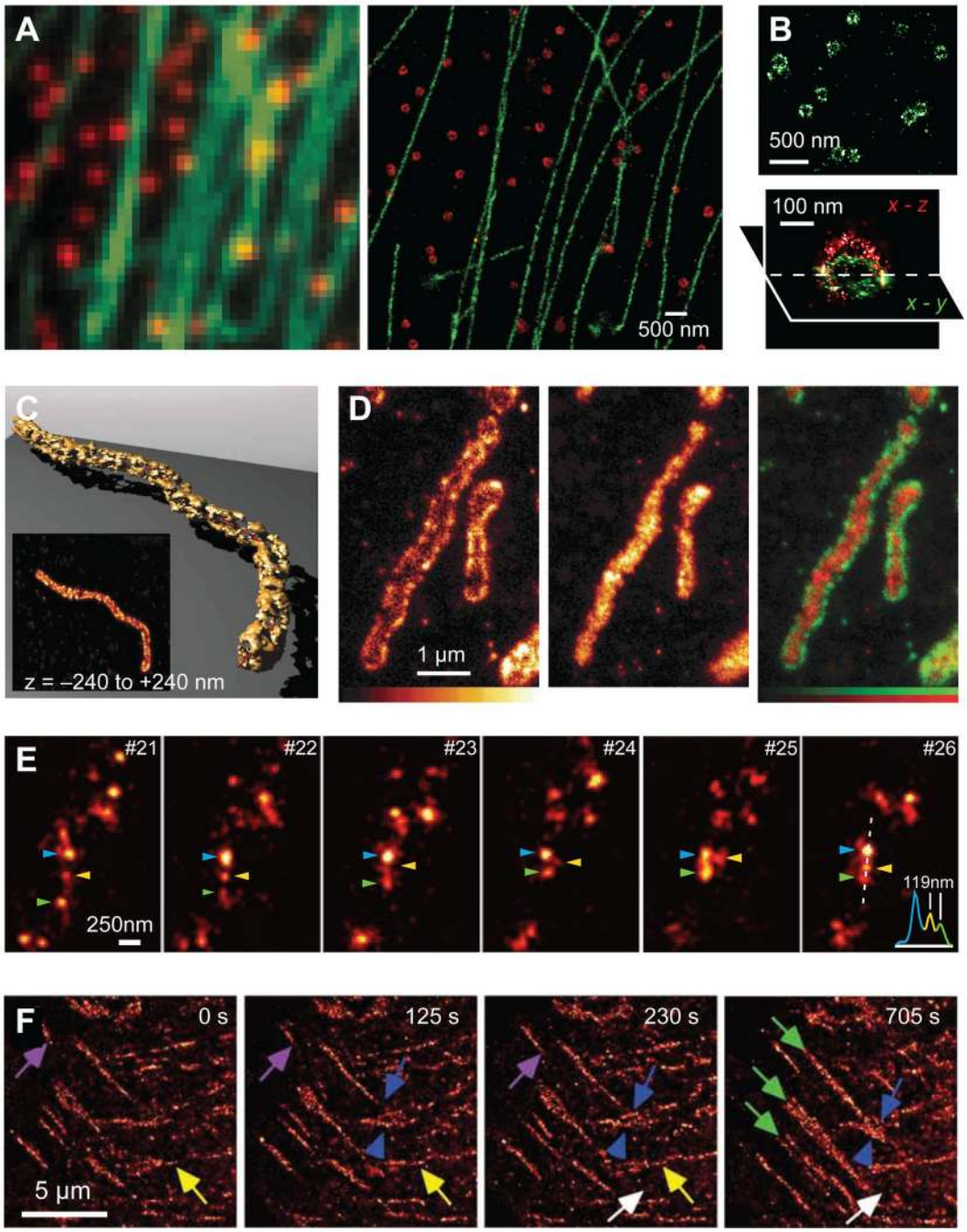

Figure 5.

Examples of super-resolution images of biological samples. (*a*) Two-color STORM imaging of immunostained microtubule (*green*) and clathrin-coated pits (*red*) (From Reference [46]. Reprinted with permission from AAAS). Microtubules overlapped in the conventional fluorescence image (*left panel*) are resolved in the super-resolution image (*right panel*). Clathrin-coated pits and microtubules with substantial colocalization in the conventional fluorescence image are clearly separated. (*b*) 3D STORM images of clathrin-coated pits (From Reference 52). Reprinted with permission from AAAS). Although shown as filled circles in the 2D STORM image (*left panel*), the 100-nm thick *x-y* section across the rim of two clathrin-coated pits (*center panel*), and the 3D perspective of a 50-nm thick *x-y* and a *x-z* section of one

pit (*right panel*) reveal their hemispherical cage shape. (*c*) 3D two-color STED microscopy of the mitochondria outer membrane immunostained for the tom20 protein (*left panel*) and the mitochondria matrix immunostained for the matrix protein Hsp60 (*center panel*) (Reprinted by permission from Macmillan Publishers Ltd.: *Nature Methods*, Reference [56], copyright 2008). In the two-color overlaid image of the 45-nm thick *x-y* section (*right panel*), the outer membrane tom20 proteins (*green*) are shown to enclose Hsp60 (*red*). (*d*) STED images of synaptic vesicles in live neurons at a frame rate of 28 fps (From Reference [64]. Reprinted with permission from AAAS). A spatial resolution of ~60 nm allows individual immunostained synaptic vesicles (*arrow heads*) to be resolved and tracked. (*e*) Live-cell imaging of a focal adhesion complex (Reprinted by permission from Macmillan Publishers Ltd.: *Nature Methods*, Reference [65], copyright 2008). Super-resolution PALM images of EosFP-tagged paxillin are reconstructed at 60-s interval. Focal adhesion complexes with different modes of movement are marked with colored arrows.

Table 1

Photoswitchable fluorophores used in super resolution fluorescence microscopy

Fluorophore		Activation wavelength (nm)	Before activation		After activation		Reversible	Reference
			Ex[a] (nm)	Em (nm)	Ex (nm)	Em (nm)		
Cyan/dark -to-green FP	PA-GFP	405	400	517	504	517	No	(88)
	PS-CFP2		400	468	490	511		(89)[b]
Green-to-red FP	Kaede	405	508	518	572	582	No	(90)
	EosFP	405	505	516	569	581		(91)
	Dendra2	405--488	490	507	553	573		(92)[b]
Dark-to-red FP	PAmCherry	405	NF		564	595	No	(62)
Reversible FP	Dronpa	405	NF		503	518	Yes	(93)
	Dronpa2				486	513		(94)
	Dronpa3				487	514		(94)
	rsFastLime				496	518		(95)
	bsDronpa				460	504		(61)
	EYFP	405	NF		513	527		(66)
Caged dyes	Caged fluorescein	<405	NF		497	516	No	*c*
	Caged Q-rhodamine[d]				545	575		
Cyanine dyes	Cy5 & Alexa 647	350--570[e]	NF		647	665	Yes	(46,58)
	Cy5.5				674	692		
	Cy7				746	773		
Photochromic rhodamine	SRA545	375	NF		Green	545	Yes[f]	(59,96)
	SRA552					552		
	SRA577					577		
	SRA617					617		

[a] commercial product of reactive fluorophore discontinued

[b] depending on the attached activator dye

[c] thermal relaxation to the dark state